



Published in final edited form as:

*Ann N Y Acad Sci.* 2008 March ; 1123: 126–133. doi:10.1196/annals.1420.015.

## Linking Cellular Energetics to Local Flow Regulation in the Heart

**James B. Bassingthwaighe**

Department of Bioengineering, University of Washington, Seattle, Washington, USA

### Abstract

A mathematical model has been developed to explain the metabolic and energetic responses induced by abnormal routes of cardiac excitation. For example, in left bundle branch block (LBBB), both glucose uptake and flow are reduced in the septal region, similar to the situation in dogs paced at the right ventricular outflow tract. In these conditions the septum is activated early, the sarcomere lengths shorten rapidly against low left ventricular (LV) pressure, and the blood flow to the interventricular septum diminishes. In contrast, the work load and the blood flow increases in the later-activated LV free wall. To provide a logical, quantitatively appropriate representation, the model links: (1) the processes of excitation–contraction coupling; (2) regional ATP utilization for force development at the cross-bridge, for ion pumping, and for cell maintenance; (3) the regulation of demands on local fatty acid and glucose metabolism for ATP generation by glycolysis and oxidative phosphorylation; and (4) feedback regulation of blood flow to supply substrate and oxygen. The heart is considered as a cylinder composed of two parts: an early-activated region and a late-activated region in tandem, but activated separately with the time delay representing the time for excitation to spread from septum to free wall. The same model equations and parameter sets are used for the two regions. The contraction of the early-activated region stretches the other region, with the result that the early-stimulated region has diminished oxygen requirements compared to those found with simultaneous stimulation. The late-activated region has increased work and increased oxygen consumption, as seen in the intact heart. Integrating the modeling of cardiac energy metabolism with local blood flow regulation and capillary–tissue substrate exchange provides a quantitative description, an hypothesis formulated to stimulate further experimentation to test its validity. The hypothesis “explains” observations of contraction and metabolism in LBBB, but whether this concept can be extended to explain the normal flow heterogeneity in the heart remains unknown.

### Keywords

myocardial blood flow; heterogeneity; cardiac pacing; excitation–contraction coupling; cellular energetics; cardiac cell model; bundle branch block; shortening deactivation; ionic regulation; smooth muscle receptors; branch point competition; apparent cooperativity

### Introduction

Left bundle branch block (LBBB) in humans<sup>1</sup> and right ventricular (RV) outflow tract pacing in dogs<sup>2</sup> result in changes in regional blood flows and metabolism. In the early-activated regions glucose uptake and flow were both reduced. The early activation initiates rapid local contraction, shortening regional sarcomere lengths without initially raising left ventricular (LV) pressure significantly. In LBBB septal blood flow was reduced, while in the late-activated

---

Address for correspondence: Prof. James B. Bassingthwaighe, M.D., Ph.D., Department of Bioengineering, University of Washington, Seattle WA 98195-5061. Voice: 206-685-2012; fax: 206-685-3300. jbb@bioeng.washington.edu.

#### Conflict of Interest

The author declares no conflicts of interest.

LV free wall, flow increased. Further, in both the humans with LBBB and the dogs chronically paced at the RV outflow, the septal wall became thinner, while the late-activated LV regions thickened by as much as 40%.<sup>3</sup> In the paced dogs, the LV free wall was initially passively stretched by the contraction of the early-activated regions before it was electrically excited, and it contracted against the developing LV pressure. The result was that the pre-stretch was followed by a prolonged, more forceful contraction, presumably due to the combination of the Starling effect and the increased afterload.

The present model links an integrated set of events: (1) the processes of excitation–contraction coupling; (2) the regional ATP utilization for force development at the cross-bridge, ion pumping, and cell maintenance; (3) the regulation of demands on local fatty acid and glucose metabolism for ATP generation by glycolysis and oxidative phosphorylation; and (4) feedback regulation of blood flow to supply substrate and oxygen. This model is of a severely reduced form, focusing on the relationship between the shortening strain, strain velocity, stress, and the local blood flow in a two-element model of heart. The two elements represent the early- and late-activated portions of the LV, arranged in tandem so that each pulls upon the other. The link between the contractile events and regional flow is mediated through local metabolic demands, consumption of substrates and oxygen used to form ATP. The inference is that in regions where there is high demand there is, at least transiently, sufficient ATP breakdown in excess of the mitochondrial capacity for the rephosphorylation of ADP to provide a vasodilatory signal. A feature of the hypothesized relationship takes into account the ultrasensitivity of vascular vasodilatory responses to interstitial adenosine,<sup>4</sup> that is, the observation that the coronary blood flow increase versus the adenosine concentration is switch-like, having a Hill coefficient of around 7.5.

## The Model

### The Regional Contraction Model

The ventricular contraction model is a two-segment heart, as if the ventricle were made up of two half cylinders, one activated before the other. No parametric differences between early and late-activated regions were used to portray the steady state of asynchronous activation in this two part “ventricle.” Instead, the model uses a single parameter set for the two regions linked in tandem, but activates them separately. The time delay from one to the other represents the time for excitation to spread from the LV septum to the free wall. The early activation of one half stretches the other, and the stronger contraction of the late-activated, pre-stretched region opposes continued contraction of the early-activated region. The model allows exploration of these questions: (a) What reduction of ATP consumption occurs with shortening deactivation in the early-activated part? Is the reduction enough to explain the observed diminutions in flow and substrate uptake? (b) What is the magnitude of the Starling effect in increasing force, ATP consumption, and blood flow in the late-activated part? (c) What does it take to make a contractile two-element model stable? The incentive for this last question is that the standard Huxley contractile sarcomere is inherently unstable in the situation diagrammed in Figure 1, even though it is normally found that sarcomere lengths in stimulated heart or skeletal muscle shorten together. The Huxley model increases the power of its contraction with increasing overlap of thick and thin filaments, so that if one segment shortens an iota stronger or a millisecond earlier than the other, then it wins the tug of war and shortens by lengthening the delayed sarcomere in tandem with it.

Of the several models that could be chosen for the contractile element, we chose the four-state model of Landesberg and Sideman,<sup>5</sup> in which the rate of formation of the strong ATP-bound state decreases as a function of the shortening velocity, and where the rate of transformation from the strong to the weak state is increased with faster shortening. If shortening is very rapid, against little load (i.e., near maximum shortening velocity), then ATP hydrolysis is reduced

compared to the rate of hydrolysis with a slower velocity of shortening when there is a higher load. This phenomenon is known as shortening deactivation. Shortening deactivation, which occurs in the early-activated septum in LBBB, then provides an explanation for the observed diminution in local blood flow and reduced glucose consumption in the septum. The corollary is that the more highly stressed, slower contracting LV free wall works harder, consuming more substrate and ATP, and demands more flow.

### **The Model for Purine Metabolism in Cardiomyocytes**

The cardiac responses to asynchronous activation in the two regions of the model are different because of the differential in ATP turnover rates at the cross-bridge. Presumably, activation and ion fluxes are similar in the two regions since the whole cardiac syncytium is activated. The cross-bridge hydrolysis of ATP drives the demand for production of ATP and the utilization of substrates and oxygen to supply ATP. While Beard<sup>6</sup> has built the best detailed model for mitochondrial oxidative phosphorylation, we have chosen, for reasons of simplicity, to use the stoichiometric kinetic model of cellular ATP regulation of van Beek,<sup>7</sup> which is based on the fact that the ADP levels in the cytosol and mitochondrial intermembrane space are the primary drivers for mitochondrial ATP generation. Accepting this premise as being quantitatively descriptive, even though it lacks Beard's mechanistic biochemical detail, we use the muscle model described in Figure 1 to drive the rate of conversion of ATP to ADP and the resultant ADP levels to drive the demand for oxygen and substrate, and to provide a byproduct critically important to the model behavior, namely the production and release of adenosine into the interstitial space. This is then used in the model module describing the receptor activation of smooth muscle vasodilatation.

van Beek's model for the mitochondrial response to ADP in the intermembrane space accounts for ATP and ADP in cytosol and intermembrane space, for the permeation of the outer mitochondrial membrane by ATP, ADP, Pi, creatine and phosphocreatine and H<sup>+</sup> ion. Taking one ADP across the inner membrane produces one ATP in return. A fixed stoichiometric relationship to the number of oxygens used completes the stoichiometric relationships, but the rate of adenosine production at low oxygen tension (low PO<sub>2</sub>) is then a function of the myokinase reaction and the activity of 5'-nucleotidase in hydrolyzing AMP to adenosine and Pi (inorganic phosphate). Since 5'-nucleotidase appears to be downregulated in ischemia<sup>8,9</sup> and the dependency of downregulation on the level of hypoxia and its duration is not at all well defined, this is an area of model and experimental exploration. Fortunately, there are data on the permeability–surface area products for adenosine in myocardial endothelial cells and cardiomyocytes,<sup>10,11</sup> both of which are needed for constraining the estimates of the intracellular concentrations.

### **The Model for Capillary–Tissue Exchange and Metabolism**

The minimal capillary–tissue exchange unit is composed of blood, endothelial cells, interstitial space, and the parenchymal cells of the organ, in this case the cardiomyocytes. Endothelial cells lining myocardial capillaries comprise about 1% of tissue volume, yet impede transport of blood solutes to the contractile cells and they take up and release substrates in competition with myocytes. Solute permeating this barrier exhibit concentration gradients along the capillary. We use here a generic model, GENTEX, to characterize blood–tissue exchanges.<sup>12</sup> GENTEX is a whole-organ model of the vascular network providing intra-organ flow heterogeneity and accounts for substrate transmembrane transport, binding, and metabolism in erythrocytes, plasma, endothelial cells, interstitial space, and cardiomyocytes. Its primary use has been in the analysis of data from positron tomographic imaging and magnetic resonance imaging for the estimation of regional flows and metabolism. The model for purine nucleoside metabolism has been characterized via the analysis of multiple tracer indicator-dilution data

from the isolated Krebs–Henseleit-perfused non-working hearts, accounting for uptake and metabolism in myocytes and endothelial cells.

The blood–tissue exchange unit is described by partial differential equations for each of the five regions, solved by special numerical techniques<sup>13</sup> to account for the convection along the capillary, diffusional spreading of the solutes within capillary and interstitium, transmembrane transport through specialized transporters,<sup>10,11</sup> and the intracellular reactions. For this “heart model,” the standard GENTEX model<sup>12</sup> has been modified to allow for variable flow, complicating the numerical methods, but essential to defining the differential responses in the two halves of the cardiac contractile model. For the variable flow, a Mac-Cormack solver was chosen from amongst the solvers available within JSim.

### Modeling the Regulation of Arteriolar Resistance

The transmembrane transport of adenosine is directly related to the regulation of the capillary blood flow during hypoxia, where it is a powerful vasodilator acting through A<sub>2</sub> receptors on vascular smooth muscle cells of the arterioles. Presumably this is a direct local effect since cardiomyocytes surround the terminal arterioles, and the diffusion distances to the smooth muscle cells are less than a micron.

While it is understood that vasomotor control is still a research forefront, specific metabolites (lactate, H<sup>+</sup> ion, CO<sub>2</sub>), K<sup>+</sup> released from myocytes, and heightened interstitial osmolarity all play a role. Under conditions of increased cellular work and energy demand, there is also release of purine nucleosides and nucleotides that reach the adenosine receptors on smooth muscle cells to cause vasodilatation. The interesting peculiarity of the situation is that competition between the high-affinity receptors and high-capacity, lower-affinity transporters on the neighboring endothelial and myocardial cells results in the relationship between blood flow and adenosine concentration being shifted dramatically. The result is the shift to a higher apparent K<sub>d</sub> (lower apparent affinity) and a marked steepening of the slope of the flow versus [adenosine], both of these phenomena being exhibited for a single site receptor without any cooperativity; appropriate parameters result in the Hill coefficient being about 7.5, as in the data of Stepp *et al.*<sup>4</sup> Thus the modeling can and does bring the varied aspects of microcirculatory regulation together with the local ATP use.

### Mathematical Methods

Ordinary differential equations were used for the muscle and metabolic reactions. Partial and ordinary differential equations were used for the capillary–tissue exchange, and the receptor activation modeling used partial and ordinary differential equations. These were written in a convenient mathematical modeling language (MML) and the model solutions were run and displayed under JSim, our simulation interface system. The models and JSim itself are available for free download <<http://www.physiome.org>>. Modules of the transporters, pumps, ionic exchanges, capillary–tissue exchange, and some components of the metabolic components are available at this site, and are described in detail there.

### Results

Given that the likely initiating events defining the regional flow heterogeneities in the heart are at the level of the metabolic requirements to support contraction, the magnitude of the effects of asynchronicity is critical. Our model is focused on timing events, and it will be important later to take it to a second level to account for differences regionally in initial sarcomere lengths and in the degree of pre-stretch induced by contraction elsewhere.

The behavior of the two-element heart model is shown in Figure 2 for 200-ms asynchrony in calcium release. Each element consists of a contractile element in parallel with a viscous damping resistance and an elastic element. The elastic element is itself sufficient to effect stability if the Young's modulus is sufficiently high, although it cannot be so high that the muscle cannot contract, and it must be fairly low in order to allow the observed levels of shortening of 10% or so. The onset of contraction in the second element quickly brings the shortening of the first element to a stop, then forcefully lengthens it toward its rest length. As the second element has the same duration of calcium release, it continues to contract after the first element's contraction ceases, with the result that the first element is stretched to a length greater than its rest length, shown by the thinner black curve lying above 0.0 from about 0.7 to 1.3 s in the plot. The overall shortening of the second, pre-stretched element, is greater than that of the first element, even though this model's equations do not include any Starling effect. The maximum strain of element two is about 0.2, while that of element 1 is only about 0.15. (Strain is defined as the fractional length change relative to the initial length.)

These changes of length, represented by the velocities of shortening and lengthening, were translated into ATP use through the equations for the reaction rates for the Landesberg–Sideman model, a four-state model for the Ca-bound and unbound forms of troponin-C and the activation (or not) of the strong versus weak form of the Ca-bound form. The assumption was that the rate of ATP use depended not only on the concentrations of the reactants, but also on the shortening velocity itself, as Landesberg and Sideman<sup>5</sup> also considered, the ATP hydrolysis rate decreasing with increasing shortening velocity, describing the decreased likelihood of cross-bridge attachment and ATP turnover when the myosin heads move too rapidly to bind to the attachment sites on the actin. The result is that more ATP, and therefore oxygen, is used by the late-activated element, as is shown in Figure 3.

Intermediate in the system, lying between the contractile events and the flow responses, is the metabolic network and its regulation. This concerns the utilization of substrates, the shifts to downregulate glucose utilization in the early-activated regions and upregulate it in late-activated regions, the balance between glucose and fatty acid use, and, over the longer term, the regulation of transcription of contractile proteins, and of the growth of capillaries in the late-activated regional subject to regional hypertrophy.

### Linking Local Metabolism to Local Flow

There are multitudinous factors involved in vasoregulation, and in this modeling approach we attempt only to give an example of the kind of influences at play, focusing on the observations of Stepp *et al.*<sup>4</sup> that the relationship between plasma adenosine concentration and coronary blood flow is switch-like: the Hill coefficient for the plot of flow versus plasma [adenosine] is about 7.5.

Figure 4 shows the fractional occupancy of a receptor with a single binding site, and no cooperativity, as a function of the concentration in the ISF and in the capillary plasma. The geometry of the model is normal: a capillary bounded by a permeable capillary wall, a surrounding interstitial fluid region (ISF), and a receptor within the ISF. The receptor has a high affinity for adenosine, and is in competition with low-affinity reaction sites consuming adenosine, for example, ISF adenosine deaminase or the adenosine transporters on the neighboring cells, which are low-affinity sites but in high concentrations. The interesting thing is that the presence of the low-affinity competitors transforms the receptor activation from a standard Michaelis–Menten relationship with a Hill coefficient of unity into almost switch-like activation.

Figure 4 shows in the four curves to the left, the relationship of site occupancy to the local adenosine concentration at four different rates of association of agonist to receptor. At a fast

rate of binding,  $K_{onR} = 10/\text{sec}$ , and the binding curve is close to the curve for equilibrium dissociation, but the apparent  $K_D$  is about  $2 \cdot 10^{-3}$  or twice the actual  $K_D$  (dotted left-most curve). At slower binding rates (with the same  $K_D$ ), the binding curves are shifted strongly rightward (apparent lower affinities) and the curve become steeper (higher effective Hill coefficients).

The four curves to the right show the relationships between fractional occupancy,  $RA/R_{tot}$ , and the driving concentration in the plasma. What is particularly interesting is that *all* four curves have a high Hill coefficient, and that binding to the receptor is resulting in switch-like behavior from the point of view of the plasma concentrations. Since the ISF concentration cannot normally be observed, this is what counts. The results show that the data of Stepp *et al.*<sup>4</sup> showing the Hill coefficient of 7.5 can be explained in terms of a noncooperative receptor binding of a single agonist molecule. Secondly, the rate of agonist binding has relatively little influence; at the fastest association rate,  $10/\text{s}$ , the apparent  $K_D$  is 25 mM, and with  $K_{onR}$   $10^4$  slower, the apparent  $K_D$  is only 4 times higher, not  $10^4$ .

The general result follows from this illustration of behavior in Figure 4: whenever a high-affinity binding site (enzyme, transporter, receptor, simple binding site) is situated behind a membrane or in a location where there is slow access to the site, the presence of a lower-affinity, high-capacity site in the neighborhood will shift the behavior of the *system* in a fashion that the binding site appears to demonstrate cooperativity (a high Hill coefficient) and to be operating with a much reduced affinity (a higher  $K_D$ ). This obviously is a warning concerning the interpretation of data suggesting cooperativity.

## Discussion

At this point in the development of the concept, the computer modeling shows that a rational conceptual basis for the normal heterogeneity of flow may be based on local differences in a variation in local work loads within the myocardium. There are many further steps to be taken before this can be regarded as the *accepted* working hypothesis.

The evidence from the heterogeneity of fatty acid uptake<sup>14</sup> is strong because those data can only be explained by specialized mechanisms for either uptake or retention of isotopically labeled fatty acid, and an alternative hypothesis of passive uptake and retention is rejected by the modeling analysis. High-flow regions required much greater transport or reaction capacity than low-flow regions, implying that specific proteins (transporters or enzymes) had much higher expression levels in the high-flow regions.

The same case might be made for the oxygen data—that is, high-flow regions required more oxygen, except in this case it is not proven that expression levels of mitochondrial proteins involved in oxidative phosphorylation are expressed to higher levels in high-flow regions. This is something that might be examined.

Another test of the hypothesis would be to obtain at higher spatial resolution the evidence relating local work load to substrate uptake. Ultrasound measures of local strain, coupled into three-dimensional model interpretation in terms of work, coupled with evidence of local oxygen consumption, would strengthen the evidence in favor of the idea.

The modeling discussed here is not definitively described, in the sense that the detailed equations, the justifications for them, the validation against experimental data on a time-point by time-point basis, have not been provided. Thus the requirements set forth for modeling, defined as a set of proposed standards for publishing models and put forward on the website <[www.physiome.org/Models](http://www.physiome.org/Models)>, are not fulfilled. However, the individual components are available as modules on that website, and can be built upon by other investigators.

## Conclusions

The anatomic–physiologic basis for the broad heterogeneity of regional blood flows observed in the normally functioning healthy heart is based on innate heterogeneity of contractile workload. More work requires more ATP formation, more substrate, and the delivery of more oxygen and substrate to the higher-flow regions. The modeling predicts that increases in ATP turnover rates result in increased local flow, which makes good sense with transitions from rest to exercise or exerting stronger contractions in any particular region. The model, lacking any description for the regulation of transcription, fails of course to predict the long-term adaptations that occur in the LV free wall subsequent to initiating LBBB, namely hypertrophy and an increased ratio in the number of capillaries per cardiocyte. Further data to test these concepts is needed.

## Acknowledgments

The author's research has been supported by NIH Grants HL19139 (for the heterogeneity studies) and RR01243 and BE01973 (for the development of JSim), and by NSF Grant 0506477 and an NIH grant for the multiscale model designing.

## References

1. Althoefer C. Editorial: LBBB: challenging our concept of metabolic heart imaging with fluorine-18-FDG and PET. *J Nucl Med* 1998;39:263–265. [PubMed: 9476933]
2. Prinzen FW, Augustijn CH, Arts T, et al. Redistribution of myocardial fiber strain and blood flow by asynchronous activation. *Am J Physiol (Heart Circ Physiol)* 1990;259:H300–H308.
3. Van Oosterhout MFM, Arts T, Bassingthwaighte JB, et al. Relation between local myocardial growth and blood flow during chronic ventricular pacing. *Cardiovasc Res* 2002;53:831–840. [PubMed: 11922893]
4. Stepp DW, van Bibber R, Kroll K, Feigl EO. Quantitative relation between interstitial adenosine concentration and coronary blood flow. *Circ Res* 1996;79:601–610. [PubMed: 8781493]
5. Landesberg A, Sideman S. Force-velocity relationship and biochemical-to-mechanical energy conversion by the sarcomere. *Am J Physiol Heart Circ Physiol* 2000;278:H1274–H1284. [PubMed: 10749725]
6. Beard DA. A biophysical model of the mitochondrial respiratory system and oxidative phosphorylation. *PLoS Comput Biol* 2006;1:e36, 0252–0264. [PubMed: 16163394]
7. van Beek JHGM. Adenine nucleotide-creatine-phosphate module in myocardial metabolic system explains fast phase of dynamic regulation of oxidative phosphorylation. *Am J Physiol Cell Physiol* 2007;293:C815–C829. [PubMed: 17581855]
8. Gustafson LA, Kroll K. Down regulation of 5' nucleotidase in rabbit heart during coronary underperfusion. *Am J Physiol Heart Circ Physiol* 1998;274:H529–H538.
9. Gustafson LA, Zuurbier CJ, Bassett JE, et al. Increased hypoxic stress decreases AMP hydrolysis in rabbit heart. *Cardiovasc Res* 1999;44:333–343. [PubMed: 10690310]
10. Schwartz LM, Bukowski TR, Revkin JH, Bassingthwaighte JB. Cardiac endothelial transport and metabolism of adenosine and inosine. *Am J Physiol Heart Circ Physiol* 1999;277:H1241–H1251.
11. Schwartz LM, Bukowski TR, Ploger JD, Bassingthwaighte JB. Endothelial adenosine transporter characterization in perfused guinea pig hearts. *Am J Physiol Heart Circ Physiol* 2000;279:H1502–H1511. [PubMed: 11009434]
12. Bassingthwaighte JB, Raymond GR, et al. GENTEX, a general multiscale model for *in vivo* tissue exchanges and intraorgan metabolism. *Phil Trans Roy Soc A: Math Phys Eng Sci* 2006;364:1423–1442.
13. Bassingthwaighte JB, Wang CY, Chan IS. Blood-tissue exchange via transport and transformation by endothelial cells. *Circ Res* 1989;65:997–1020. [PubMed: 2791233]

14. Caldwell JH, Martin GV, Raymond GM, Bassingthwaighte JB. Regional myocardial flow and capillary permeability-surface area products are nearly proportional. *Am J Physiol Heart Circ Physiol* 1994;267:H654–H666.



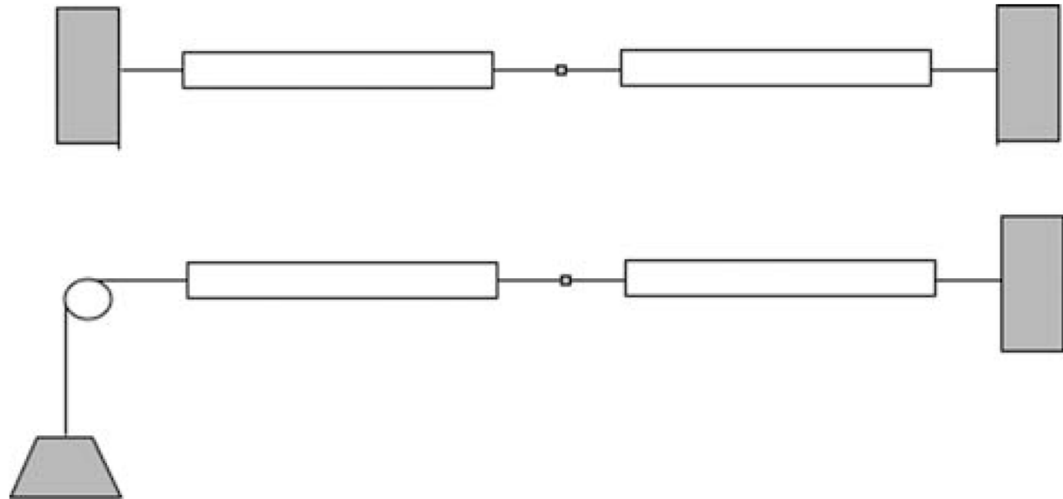


**FIGURE 1.**

Two versions of a two-sarcomere heart. *Top*: two segments in tandem, but constrained to constant length (isometric total length). In this case, early activation of one of the two, any shortening causes lengthening of the other. *Bottom*: situation allowing the total length to shorten against load, performing external work.

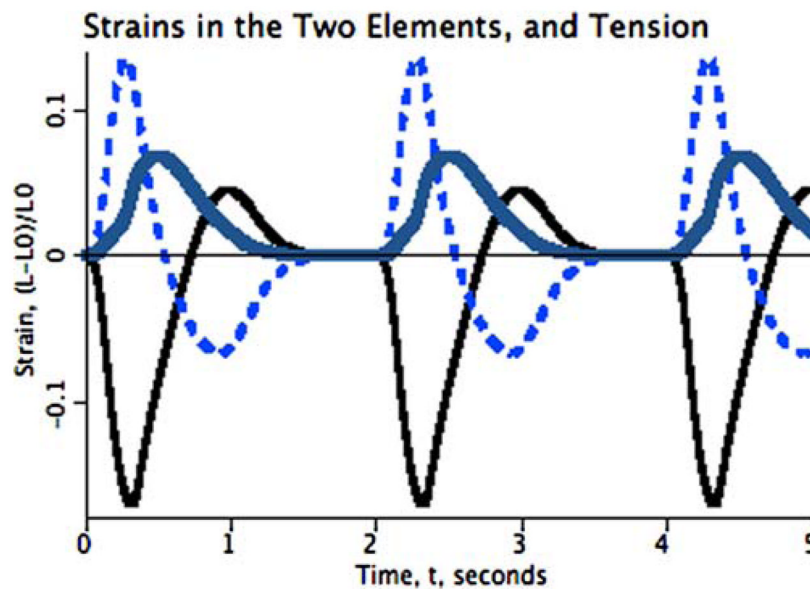


**FIGURE 2.**

Two elements contracting in tandem: The model is driven by a stimulus releasing a wave of increased calcium concentration, thereby allowing the formation of cross-bridges between actin and myosin, the hydrolysis of ATP, and the development of contractile force and shortening. Three cycles are shown. Shortening of the first-stimulated segment (*continuous thin trace*) is slowed by stretching the series elastic element in the second (*dashed trace*) until it begins to contract at about 0.2 s after the first. The series elasticity prevents the stretching of the second segment from being so great that actin–myosin overlap goes to zero, so the second element does develop force. Parameters for the two elements are identical, the only difference being that one is stimulated 200 ms earlier than the other. Development of pressure is represented by the rise in tension (*thick curve*), lifting the weight in the diagram in bottom part of Figure 1, resulting in a tension waveform analogous to that of LV cavity pressure.

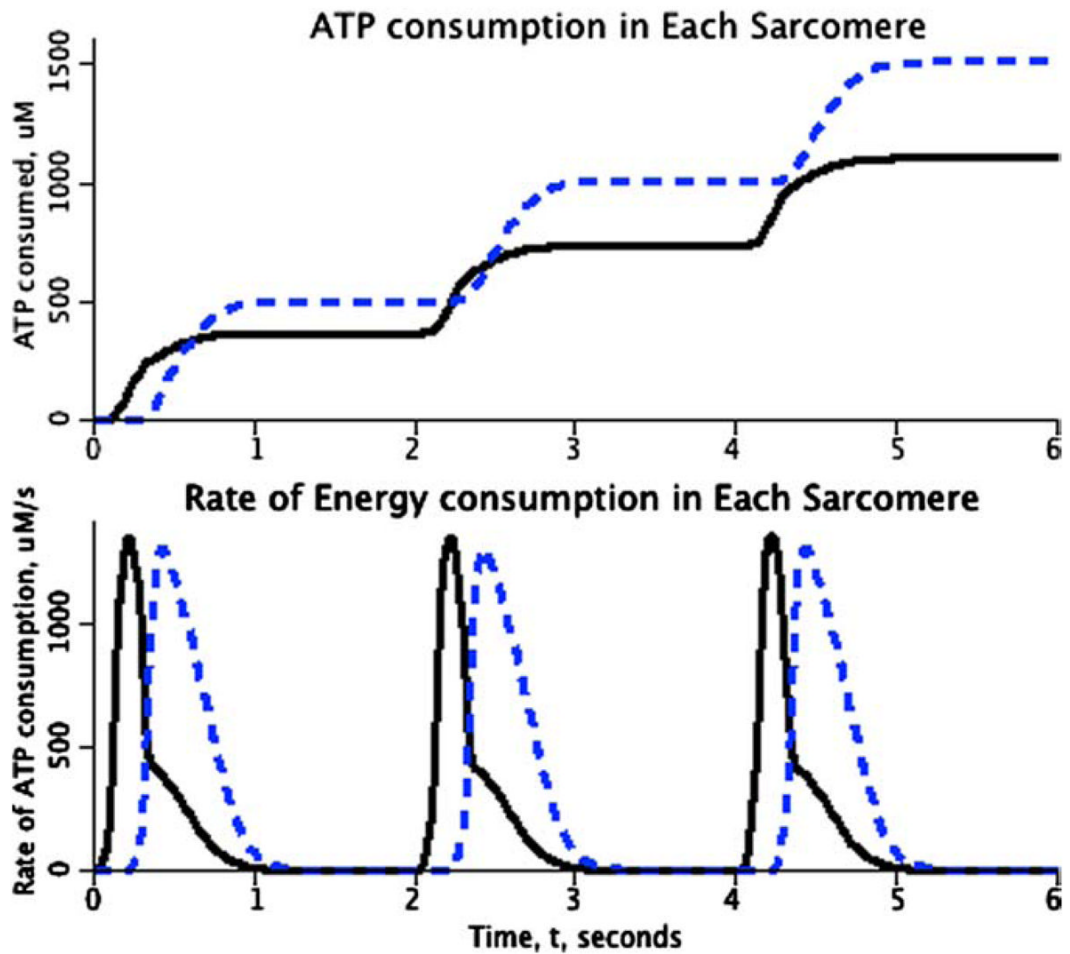


**FIGURE 3.**

Energy utilization in a pair of asynchronously activated elements in series. (Parameters identical to those used for Fig. 2.) *Lower panel:* Rate of ATP hydrolysis by the first-stimulated (*continuous curve*) and second-stimulated (*dashed*) elements of the two-element heart. Although the contraction of the second element prolongs the ATP turnover of the earlier-contracting element, the area under the energy consumption curve is greater for the second element. *Upper panel:* The cumulative ATP use is higher in the late-activated element (*dashed curve*) compared to that of the early-activated element (*continuous curve*), even though both have exactly the same parameters.

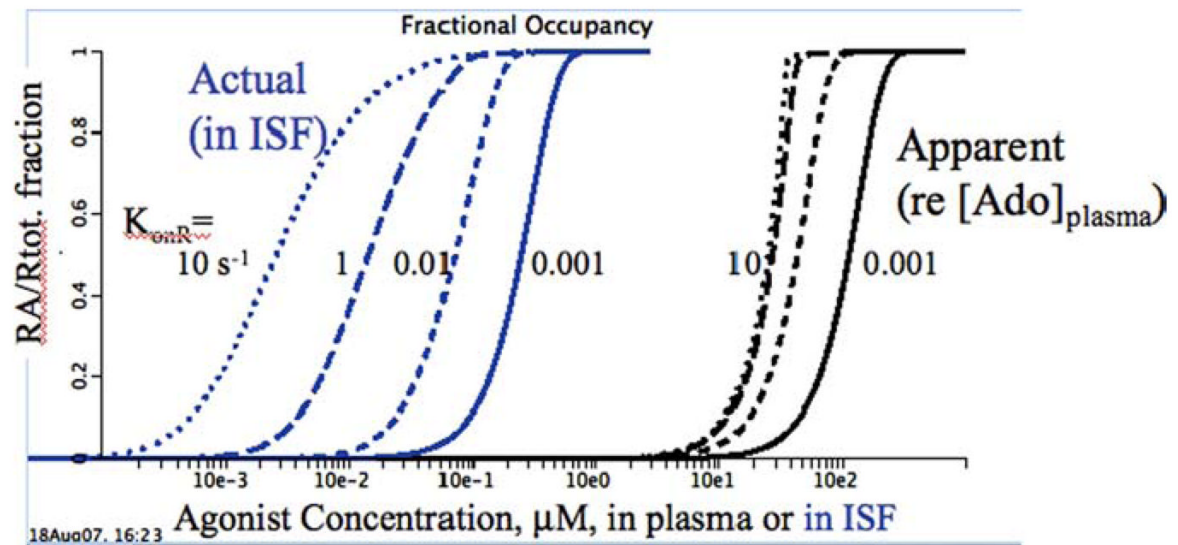


**FIGURE 4.**

Receptor fractional occupancy,  $RA/R_{tot}$ , for an interstitial receptor, when there is hindered delivery of the agonist and competition for it from lower-affinity transporters and enzymes in the interstitial space (ISF). Agonist was delivered at high flow into the plasma space with a slowly rising concentration and permeated the capillary with a PS of  $0.2 \text{ mL}/(\text{g}\cdot\text{min})$ . The actual receptor  $K_D = 1 \text{ }\mu\text{M}$  and the competing enzyme dissociation constant  $K_E = 10 \text{ mM}$ , 10,000 times lower affinity. The four curves to the *left* show  $RA/R_{tot}$  versus interstitial concentration  $[\text{agonist}]_{ISF}$ . The group of four curves to the *right* show  $RA/R_{tot}$  versus plasma concentration  $[\text{agonist}]_{pl}$ .